

1 Title: Modeling global distribution of agricultural insecticides in surface waters

2
3 Authors: Alessio Ippolito^{a,b}, Mira Kattwinkel^{c,d}, Jes J. Rasmussen^{c,e}, Ralf B. Schäfer^f, Riccardo
4 Fornaroli^b, Matthias Liess^{c,1}

5 Affiliations:

6 ^a International Centre for Pesticides and Health Risk Prevention, L. Sacco University – Hospital, Via G.B. Grassi, 74,
7 20157, Milan, Italy.

8 ^b Department of Earth and Environmental Sciences (DISAT), University of Milano - Bicocca, Piazza dellaScienza 1,
9 20126, Milan, Italy.

10 ^c UFZ, Helmholtz Centre for Environmental Research, Dept. System-Ecotoxicology, Permoserstrasse 15, 04318
11 Leipzig, Germany.

12 ^d Department of System Analysis, Integrated Assessment and Modelling, Eawag, Überlandstrasse 133, P.O. Box 611,
13 8600 Dübendorf, Switzerland

14 ^e Department of Bioscience, Aarhus University, Vejlsovej 25, 8600 Silkeborg, Denmark.

15 ^f Institute for Environmental Sciences, University Koblenz-Landau, Campus Landau, Fortstrasse 7, 76829 Landau,
16 Germany.

17
18 ¹Corresponding Author: Alessio Ippolito

19 e-mail: ippolito.ecotox@gmail.com

20 Telephone: +39 333 5865622

21
22 **Abstract:** Agricultural insecticides constitute a major driver of animal biodiversity loss in
23 freshwater ecosystems. However, the global extent of their effects and the spatial extent of exposure
24 remain largely unknown. We applied a spatially explicit model to estimate the potential for
25 agricultural insecticide runoff into streams. Water bodies within 40% of the global land surface
26 were at risk of insecticide runoff. We separated the influence of natural factors under human control
27 determining insecticide runoff. In the northern hemisphere, insecticide runoff presented a latitudinal
28 gradient mainly driven by insecticide application rate, in the southern hemisphere, a combination of
29 daily rainfall intensity, terrain slope, agricultural intensity and insecticide application rate
30 determined the process. The model predicted the upper limit of observed insecticide exposure
31 measured in water bodies (n=80) in five different countries reasonably well. The study provides a
32 global map of hotspots for insecticide contamination guiding future freshwater management and
33 conservation efforts.

34 Key words: Insecticide runoff, Exposure models, Risk assessment, Global map

35
36 **Capsule:** We provide the first global map on insecticide runoff to surface water predicting that
37 water bodies in 40% of global land surface may be at risk of adverse effects.

38
39 **Highlights:**

- 40 • first global map on insecticide runoff through modelling
41 • model predicts upper limit of insecticide exposure when compared to field data
42 • water bodies in 40% of global land surface may be at risk of adverse effects
43 • insecticide application rate, terrain slope and rainfall main drivers of exposure

44 **Introduction**

45 An estimated 2.3×10^6 tons of pesticides are annually applied to agricultural land at the global scale
46 (Grube et al., 2011) to maintain high levels of production. This amount is equivalent to an annual
47 application of 0.15 kg of pesticide per hectare of the total land surface of the earth. The
48 environmental effects caused by these substances are fundamentally different from those of other
49 classes of chemicals, as pesticides are intentionally designed and released into the environment to
50 eradicate pests and weeds. Consequently, pesticides are a major threat to terrestrial (Barmaz et al.,
51 2010; Boatman et al., 2007; Newton, 1995) and aquatic biodiversity (Liess & von der Ohe, 2005;
52 Relyea, 2005; Schäfer et al., 2012; Verro et al., 2009), although the global extent of their effects
53 remains largely unknown. Similarly, the relative importance of main factors driving the exposure at
54 a global scale needs further research. Studies performed at the local and regional scale have
55 demonstrated that agricultural practices (Brown et al., 2008; Tang et al., 2012) and landscape
56 features (Schriever et al., 2007) determine the magnitude of exposure. Large-scale screening
57 approaches, such as spatially explicit models based on Geographic Information Systems (GIS),
58 allow for rapid and cost-effective exposure estimations (Schriever et al., 2007). The identification
59 of areas of concern can trigger regional monitoring programs and, if necessary, exposure mitigation
60 measures.

61 Given that insecticides are designed to control pest insect populations, they have the
62 potential to impair aquatic invertebrate populations, which play a major role in aquatic ecosystem
63 structure and functioning (Fleeger et al., 2003; Ippolito et al., 2012; Liess & Beketov, 2011; Liess &
64 von der Ohe, 2005; Schäfer et al., 2012). Such estimation of the current state of insecticide
65 contamination in freshwater bodies is pivotal for a targeted conservation and restoration of these
66 ecosystems in order to achieve a satisfactory ecological quality. The need for a global scale
67 perspective is at present particularly essential because farmers in many developing countries are
68 changing from traditional subsistence farming to market-oriented intensive-crop farming

69 (Satapornvanit et al., 2004). Moreover, global climate change is proposed to result in a significant
70 increase in the global insecticide application on crops, especially in industrialized countries (Boxall
71 et al., 2009; Kattwinkel et al., 2011).

72 Several field studies documented that most insecticides can enter surface water bodies via
73 surface runoff triggered by heavy rain episodes (Van der Werf, 1996; Wauchope, 1978). In this
74 study we used existing raster maps (FAO & IIASA, 2006; Batjes, 2006) and spatial databases
75 (NOAA; FAO) as input data for a spatially explicit model (Kattwinkel et al., 2011; Schriever &
76 Liess, 2007; Schriever et al., 2007) estimating the surface Runoff Potential (RP) following strong
77 rainfall events. This RP model (Eq. 1) used to estimate insecticide input into streams, was split into
78 two parts to separate environmental factors (e.g. daily rainfall intensity, soil characteristics, slope of
79 the terrain etc.), from human-controlled variables (due to agricultural practices) that determine
80 insecticide runoff. Subsequently, the predictions of the model were compared to monitored peak
81 flow measurements of insecticide contamination in streams of four different biogeographic regions.

82 **Materials and Methods:**

83 ***Model***

84 We used a generic indicator (RP; runoff potential) that distinguishes stream sites based on
85 key characteristics of the environment around the stream to assess the potential for insecticide
86 runoff inputs (Kattwinkel et al., 2011; Schriever & Liess, 2007; Schriever et al., 2007). The RP is
87 based on a mathematical model (Eq. 1) that estimates the amount (gLOAD) of a generic substance
88 that was applied in the near-stream environment and that may reach the stream in response to a
89 single rainfall event.

$$90 \quad \text{gLOAD}_i = \frac{D \cdot A_i \cdot K_{OC} \cdot \left(\frac{1}{1 + K_{OC}} \right)}{100} \quad (\text{Eq. 1})$$

91 The model equation is built on nine parameters. i : grid cell index; A_i : area [ha] of the stream
92 corridor; D : country-specific insecticide application rate [$\text{g}\cdot\text{ha}^{-1}$]; K_{OC} : soil organic carbon-water

93 partitioning coefficient [adim]; OC_i : organic carbon content [%]; s_i : slope [%]; $f(s_i)$: influence of
94 slope on runoff; P_i : daily rainfall intensity [mm], T_i : texture; $f(P_i, T_i)$: volume of surface runoff due
95 to precipitation [mm]; p_i : proportion of croplands in cell i ; I : average plant interception [%].

96 All spatial calculations were performed with ArcGis 10 (ESRI, Redlands, CA, USA). The
97 grid cell size used in the study was 5×5 arc-minutes. As a result, gLOAD reflected the mean
98 generic exposure of a stream section that would be located in a cell and had the same environmental
99 characteristics as the grid cell. The RP of an individual grid cell was derived as the log10-
100 transformed gLOAD and was subsequently classified into five order-of-magnitude categories (RP
101 values as class boundaries: -3; -2; -1; 0).

102 In addition, the model was split into two submodels: the first included all environmental
103 variables affecting the RP (daily rainfall intensity, soil characteristics, and slope); the second
104 incorporated those variables that are under human control (insecticide application rate, crop
105 interception, fraction of land used for growing crops). By analogy with the classical risk equation,
106 the first submodel was used to construct a vulnerability map, with vulnerability taken as the natural
107 degree of susceptibility to runoff in each grid cell. The second submodel was used to derive the
108 hazard associated with the human management of insecticides in agriculture. The vulnerability and
109 hazard maps show completely different ranges of variation; hence, the class boundaries for these
110 maps were assigned ex-post according to the distribution function of the values (quintiles).

111 ***Area of the stream corridor (A_i)*** - No real stream courses were considered in the present
112 study. In accordance with previous studies (Schriever & Liess, 2007; Schriever et al., 2007), for
113 each grid cell we considered a generic stream segment with one bifurcation. The near-stream
114 environment was set to an area of 45 ha, which was derived from a two-sided 100-m stream
115 corridor that extended 1500 m upstream from the site (the bifurcation was placed midway in the
116 upstream corridor).

117 ***Insecticide application rate (D)*** - Country-based data on the rate of insecticide
118 application were retrieved from the FAOSTAT database (FAO). All available data for each country

119 referring to the years 2000-2010 were considered. Issues reported in metadata (e.g. data refer to
120 imports only or data expressed in formulated products) were evaluated case by case and unreliable
121 data were discarded. A country was considered only if at least two acceptable data points were
122 present for the abovementioned period. The arithmetic mean of the insecticide application rate was
123 calculated for each country, unless the specific coefficient of variation was $> 100\%$. Then, if a clear
124 trend was observed, only the latest value was considered (most representative of the present
125 situation), else the country data was omitted. For those 84 out of 165 countries without respective
126 data, the insecticide application rate was estimated. The estimation was done using a linear model
127 with the predictors average accumulated temperature (see below), the fraction of insecticide high-
128 consuming crops, and the GDP. The average accumulated temperature was included as predictor
129 since a strong correlation between temperature and the rate of insecticide application has been
130 identified in another study (Kattwinkel et al., 2011) for European countries.

131 We calculated the average accumulated temperature for each country using a map produced by
132 FAO & IIASA (33) ($T_{\text{mean}} > 0 \text{ }^{\circ}\text{C}$), then weighting the value of each grid cell in the country by the
133 corresponding proportion p_i of croplands (taken from FAO) to account for potential differences in
134 temperature between crop and non-crop areas. The insecticide application rates may vary strongly
135 among crops. Therefore, crops were divided into two classes on the basis of their typical insecticide
136 amount requirements using the U.S. National Pesticide Use Database (Gianessi & Reigner, 2006).
137 Insecticide high-consuming crops included all kinds of fruits, nuts and olives; insecticide low-
138 consuming crops included all remaining crops (mostly cereals, vegetables, herbs and fiber crops).
139 Typical insecticide application rates differed significantly between the two groups ($p < 0.0001$,
140 Mann-Whitney and Kolmogorov-Smirnov tests). The fraction of insecticide high-consuming crops
141 in each country was estimated on the basis of the information retrieved from FAOSTAT database
142 (FAO) for the years 2000-2010. Finally, the insecticide application rate is also determined by the
143 economic situation in a country. Therefore, we also included the country-specific GDP. GDP values
144 (expressed in 2005 US dollars) per capita per country per year were retrieved from the Economic

145 Research Service's International Macroeconomic Data Set (ERC). Median GDP values were
146 calculated for all countries over the period 2000-2010. The regression model was calculated with
147 the software [R] using all the log-transformed available data at the country level. All country-based
148 rates of insecticide application were normalized by dividing them by the application rate for
149 Germany to enable comparability to those used in previous studies (Kattwinkel et al., 2011;
150 Schriever & Liess, 2007). A detailed description of the procedure to derive country-specific
151 insecticide application rate is reported in SI-I

152 *K_{OC}* - The soil organic carbon-water partitioning coefficient is substance specific. We
153 considered all insecticides with respect to the application rate, therefore a substance-specific value
154 could not be assigned. The *K_{OC}* value was set to 100 in accordance with (Kattwinkel et al., 2011;
155 Schriever & Liess, 2007). This assumption is rather worst case since most insecticides (>75% of
156 used compounds, according to our estimation) have *K_{OC}* values higher than 100, which would result
157 in lower RP. However, in the absence of detailed per country information that would allow to
158 compute an average *K_{OC}* per country, the assignment of a different value for the global *K_{OC}* would
159 not change the relative scale obtained for RP.

160 *Daily Rainfall Intensity (P_i)* - RP is determined by single rainfall events. We calculated the
161 median value of the monthly maximum precipitation for each of the 76,687 stations (over the entire
162 available period) collected in the NOAA - GHCN daily database (NOAA). We then assigned to
163 each station the maximum value within the productive season. Productive seasons were assessed
164 using two maps included in the Food Insecurity, Poverty and Environment Global GIS Database
165 (FGGD) (FAO & IIASA, 2006). First, we considered the areas in which a lack of water is the
166 principal constraint on agriculture, according to the "Hierarchical distribution of severe
167 environmental constraints map". In those areas, no time period limitations were established because
168 it is likely that the rainiest month is the period of maximum productivity. In all other areas, the
169 length of the growing period was assigned on the basis of the corresponding FGGD map (FAO &

170 IIASA, 2006), while the temporal collocation of the growing season was differentiated between the
171 northern and southern hemispheres.

172 With this methodology, we assigned one value to each of the GHCN stations for which the
173 coordinates were known. Hence, the points were interpolated over the global land surface. Several
174 (ordinary kriging) semivariogram models were tested: the choice of the final interpolation model
175 aimed at minimizing (i) the root-mean-squared prediction error and (ii) the difference between the
176 latter and the average estimated prediction standard error. The best results in terms of prediction
177 (60%, $p < 0.0001$, F-test) and uncertainty estimation were obtained with a Stable semivariogram
178 model.

179 The function $f(T, P)$ proposed by the OECD (OECD, 1998) (Eq. 2) is based on empirical values and
180 it is valid in the range of 6-100 mm. Therefore, all values of daily rainfall intensity below 6 mm or
181 above 100 mm were set to 6 and 100 mm, respectively (accounting for 1% of total grid cells).

$$182 \quad f(T, P) = \begin{cases} -5.86 \cdot 10^{-6} \cdot P_i^3 + 2.63 \cdot 10^{-3} \cdot P_i^2 - 1.14 \cdot 10^{-2} \cdot P_i - 1.64 \cdot 10^{-2} & \text{if } T_i = \text{sand} \\ -9.04 \cdot 10^{-6} \cdot P_i^3 + 4.04 \cdot 10^{-3} \cdot P_i^2 - 4.16 \cdot 10^{-3} \cdot P_i - 6.11 \cdot 10^{-2} & \text{if } T_i = \text{loam} \end{cases} \quad (\text{Eq. 2})$$

183 A detailed description of the procedure to derive daily rainfall intensity is reported in SI-II

184

185 **Plant interception (I)** - Plant interception is plant- and growth-phase specific. Nevertheless,
186 agricultural patterns (the growth phases during which plants are treated) are too complex and
187 spatially heterogeneous to be represented in a global assessment. Also, a reliable representation of
188 crop distribution patterns at global scale is not available. In the European Generic guidance for
189 FOCUS surface water scenarios (FOCUS, 2012), plant interception values corresponding to four
190 phenological stages are reported for 21 different crops. Insecticide are likely not to be applied
191 during the first stage, when interception is zero for all crops. The mean and the median of the of the
192 remaining values ($n=63$, 3 stages x 21 crops) is 0.5. Hence, a fixed plant interception value of 50%
193 was applied to each grid cell.

194 **Soil variables (T_b , OC_i)** -The values of the soil variables were retrieved from ISRIC-WISE
195 (Batjes, 2006). The organic carbon content of the first soil layer (0–20 cm) was considered. In the

196 ISRIC-WISE map, organic carbon is expressed in six classes. In our study, each cell was assigned
197 the mean value of its class rounded to the nearest integer. Texture was derived from the database
198 attached to the ISRIC-WISE map. The percentage content of clay, silt, and sand in the first soil
199 layer (0–20 cm) was used to classify the texture as sandy or loamy. Criteria for the classification
200 were retrieved from Finern et al. (2005).

201 ***Proportion of cropland in each grid cell (p_i)*** - The occurrence of cropland was taken from
202 the FGGD project (FOA & IIASA, 2006).

203 ***Slope (s_i)*** -The average slope was taken from the FGGD project (FOA & IIASA, 2006). In
204 the relevant FGGD map, slope was expressed in terms of seven classes. In our study, each cell was
205 assigned the mean value of its class rounded to the nearest integer. The function determining the
206 influence of slope on runoff according to OECD (1998) is Eq. 3

$$207 \quad f(s_i) = \begin{cases} 0.001423 \cdot s_i^2 + 0.02153 \cdot s_i, & \text{if } s_i \leq 20 \% \\ 1, & \text{if } s_i > 20 \% \end{cases} \quad (\text{Eq. 3})$$

208

209 ***Sensitivity analysis***

210 A sensitivity analysis was carried out to analyze the influence of changes in each model
211 input variable on RP scores. Model sensitivity was assessed by varying one parameter at a time in
212 the ranges +/-25% and +/- 50%, while all other parameters were kept constant at their mean values
213 (daily rainfall intensity = 28.9 mm; organic carbon = 2.17%; slope = 12.8%; fraction of cropland in
214 each cell = 0.25, calculated disregarding cells for which this fraction was zero; insecticide
215 application rate = 0.34, calculated as median among countries) or at specified values (K_{OC} =100;
216 plant interception = 50%) .

217 ***Uncertainty analysis***

218 An uncertainty analysis was performed to take into account, how estimated RP values could
219 change in response to the uncertainty of the input parameters. Uncertainty ranges were estimated for
220 each parameter in each grid cell. Values of one parameter at a time were set to the extremes of the

221 corresponding uncertainty range (lower and upper limit) and RP values were recalculated. We
222 evaluated changes in the RP classification of grid cells with respect to the original estimation.

223 Due to different data types in the input data, different approaches were used to describe the
224 uncertainty ranges. For the insecticide application rate (D), 95% prediction limits of the linear
225 model used for prediction (see above) were used as upper and lower extremes of the uncertainty
226 range for each country. For daily rainfall intensity (P_i), a prediction standard error map associated
227 with the kriging interpolation was calculated. Extremes of the uncertainty range for each grid cell
228 were calculated by adding to (upper limit) and subtracting (lower limit) from the predicted value
229 twice the prediction standard error. Extremes of plant interception (I) were set everywhere to 0-90%
230 in accordance with (FOCUS, 2012). No accuracy assessment was available for the map used to
231 estimate the proportion of cropland (p_i) in each grid cell (FAO & IIASA, 2006). However, this map
232 was originally derived from the Global Land Cover 2000 (EC-JRC, 2003), whose accuracy has
233 been assessed (Mayaux et al., 2006). We considered the higher error between the User's accuracy
234 and the Producer's accuracy for the category "Cultivated and managed areas" and we used this
235 value (27%) to estimate the extremes of the uncertainty range for each grid cell. Slope (s_i) and
236 organic carbon (OC_i) were derived from maps expressed in terms of classes (values intervals). The
237 extremes of these classes were used as the limits of the uncertainty ranges. To assess the uncertainty
238 due to soil texture (T_i), the model was applied assuming that the soil was loamy and sandy
239 everywhere. Detailed results of the uncertainty analysis are reported in SI-III

240 ***Quantile regression***

241 The predictions of the model were compared to actual measurements of insecticide
242 contamination in water bodies from previous field studies covering Germany (Liess & von der Ohe,
243 2005), France and Finland (Schäfer et al., 2007), Denmark (Rasmussen et al., 2011) and Australia
244 (Schäfer et al., 2011). The sampling campaigns were designed to catch runoff-induced
245 concentrations of the insecticides most widely used in the respective areas.

246 Measured insecticide concentrations were expressed as Toxic Units (TU), i.e. benchmarked
247 by a standard test organism (*Daphnia magna* in this case) to allow for comparison of different
248 substances. The maximum TUs per site (Liess & von der Ohe, 2005; Schäfer et al., 2013) were
249 matched with the corresponding RP values estimated for the same sites. Further information on the
250 studies and the raw TU data are provided in (Schäfer et al., 2013).

251 Quantile regression fits a continuous function through the local (with respect to the
252 independent variable) value of the quantile of a dependent variable to account for variation in the
253 quantile with the independent variable (Cade et al., 1999; Koenker & Bassett, 1978). We fitted
254 linear, exponential and logarithmic models to the data. For each model both (i) a τ -specific version
255 of the corrected Akaike Information Criterion (Koenker, 2013), ($AICc(\tau)$) and (ii) the Akaike
256 weights (w_i) (the relative likelihood of a model, given a data set and a set of models) were
257 calculated.

258 The difference between the model $AICc(\tau)$ and the minimum $AICc(\tau)$ was used to choose
259 the best-fitting model ($\Delta_i = AICc(\tau) - \min AICc(\tau)$), considering that the model with the lowest
260 $AICc(\tau)$ generally provides the better description of the data. Values of $\Delta_i \geq 2$ are suggested as a
261 threshold to exclude alternative models; values of $\Delta_i < 2$ indicate substantial support for the
262 alternative model (Burnham & Anderson, 2002; Johnson & Omland, 2004). Last, we determined
263 the best model form across the 80th, 85th, 90th percentiles by averaging w_i for each model from all
264 three percentiles model selection analyses. To test and compare the goodness of the different
265 models, the selection process was done for a modified dataset with all x values shifted to the
266 positive range. The functional form selected with w_i was recalculated on the original dataset and
267 was tested for statistical significance in terms of the probability that the slope and intercept were
268 zero (Scharf et al., 1998).

269 **Results and Discussion**

270 The predicted magnitude of insecticide runoff driven by environmental variables was
271 visualized in a vulnerability map (Fig. 1). The spatial pattern of vulnerability is determined by

272 geomorphology and climate, particularly the slope of the terrain and the maximum intensity of
273 rainfall during the crop growing season.

274 FIGURE 1

275 Subsequently, we produced a hazard map (Fig. 2) based on the anthropogenic factors that
276 influence runoff such as the rate of insecticide application, and the share of land used for
277 agriculture.

278 FIGURE 2

279 We combined the vulnerability and hazard maps into a map of predicted insecticide runoff
280 potential (RP) (Fig. 3) and we show that more than 40% of the global land area was at risk of
281 generating insecticide surface runoff to streams. Remarkably, RP values for more than 40% of that
282 fraction (18% of the global land area) were classified as high to very high. This result receives
283 support from a previous model-based study that identified pesticides as important pollutants of
284 streams and rivers globally (Vörösmarty et al., 2010).

285 FIGURE 3

286 High hazard was sufficient but not necessary to yield high RP values: more than 90% of the
287 grid cells characterized by a high (4th quintile) or very high (5th quintile) hazard resulted in RP
288 classes high or very high, but half of cells in the highest RP class did not originate from high or
289 very high hazard values. By contrast, high vulnerability was usually a prerequisite for very high RP
290 values (86% of cells in the highest RP class presented high or very high vulnerability), but did not
291 always translate into high RP classes.

292 The RP map indicated the presence of a north-south gradient in the northern countries, with
293 increasing RP towards the south throughout Eurasia. The same trend was observed from North to
294 Central America, except for the Midwestern United States. This tendency generally reflects the

295 insecticide application rate. The insecticide application rate depends strongly on average
296 temperature due to the dependency of several insect pests on the number of degree days (Herms,
297 2004). In addition, temperature is a limiting factor for the cultivation of high insecticide-consuming
298 crops (e.g. fruits, nuts, olives and ornamentals). Hence, climate change will likely increase the
299 proportional area with high and very high RP in the future, especially in the northern hemisphere
300 (Kattwinkel et al., 2011). By contrast, the RP values in the southern hemisphere showed no or only
301 slight changes in association with latitude. This probably reflects that the insecticide application
302 rate in these countries is constrained by socio-economic factors. Growing economies in several
303 parts of the southern hemisphere may soon overcome this constraint and attempt increasing their
304 food production e.g. through increasing insecticide application rates, which in turn may increase
305 proportions of land with high or very high RP in the future.

306 The relationship between measured insecticide concentrations (converted to Toxic Units
307 (TU) to enable comparison of potential ecological effects) in streams of five different countries
308 (France, Germany, Finland, Denmark, and Australia) and RP predictions was positive and linear for
309 all the considered percentiles in the quantile regression (80th, 85th, and 90th) (See SI-IV for details).
310 In ecological studies, 90th-percentile regressions have been used to estimate limiting-factor
311 relationships; i.e. 90% of the observations are below the fitted line (Konrad et al., 2008). Since our
312 sample size was relatively small (n= 80), we modeled 3 extreme percentiles (80th, 85th, 90th) for a
313 more robust analysis. The linear model consistently yielded the best goodness of fit with Δ_i always
314 greater than 10 and an averaged w_i of 0.997 (Table SI-IV 1). The positive slope of the three quantile
315 regression models indicated that the upper quantiles of the maximum logTU increased with RP (See
316 SI-IV for details). Overall, RP represents a potential - not an exact prediction of the pollution level -
317 and should be interpreted as a limiting factor that is valuable to identify potential hotspots of
318 insecticide runoff. Due to the scale used in our study, it was not feasible to consider mitigation
319 measures (vegetated buffer strips, unsprayed areas, artificial wetlands, etc.) implemented at local
320 scale. Therefore, our predictions may overestimate the exposure in regions where such measures are

321 applied. Note that measured insecticide data originated from four regions of Europe and Australia
322 and are not representative for the whole world. Nevertheless, they originated from regions with
323 considerable differences in terms of landscape and agricultural practices.

324 Several field studies reveal that the abundance of macroinvertebrates sensitive to pesticide
325 pollution decreases with increasing insecticide pollution measured during runoff episodes (Liess &
326 von der Ohe, 2005; Schäfer et al., 2007). Importantly, RP predictions for 10 km² grid cells have
327 been shown to provide reasonable predictions of abundances of sensitive macroinvertebrate species
328 from random pulls of streams in Germany, and grid cells with predicted high or very high RP
329 revealed reduced abundances of sensitive macroinvertebrate species in 55% and 90% of the
330 streams, respectively (Schriever & Liess, 2007). In the light of these results, we find it worrying
331 that we predict 18% of the global land surface having high or very high RP. Moreover, several
332 studies confirmed that undisturbed upstream sections, such as forest patches, increase recovery of
333 macroinvertebrate communities from pesticide pollution measured during storm flow (Schäfer et
334 al., 2007 and reference therein). For 60% of the area with high and very high RP values in the
335 present study, forests cover less than 20% of the surface area. Therefore, increased community
336 recovery potential facilitated by upstream forested stream sections is not expected to be high in the
337 grid cells characterized by predicted high to very high RP.

338 The sharp contrasts in some parts of the hazard map reflect national borders because: (i)
339 insecticide application rate data were averaged on a country basis and (ii) the collection, analysis,
340 and distribution of those data often vary among countries. To our knowledge, only the database
341 maintained by the Food and Agriculture Organization of the United Nations (FAO) holds data on
342 insecticide usage for most countries of the world. The insecticide rate gradient spans more than
343 three orders of magnitude. Thus, the resolution is too low to account for regional differences. In
344 addition, the insecticide use had to be estimated for 84 of the 165 countries included in the analysis
345 (linear regression model, $R^2 = 0.55$, $p < 0.001$ for full model, see methods for details), because data
346 were not available or not reliable. To our knowledge, only one other study has estimated the rate of

347 pesticide application for countries without data (Esty et al., 2005). However, that study did not
348 distinguish between insecticides, herbicides and fungicides, which is essential for the present study.

349 The sensitivity analysis revealed that the RP model was most sensitive to changes in slope.
350 In addition, the model showed a high degree of sensitivity to changes in daily rainfall intensity
351 values, whereas the organic carbon content exhibited smaller influence. Generally, a variation of +/-
352 25% in the input parameters caused an average change in RP by |0.08| to |0.18|. A variation of +/-
353 50% in the input parameters would result in an average change in RP by |0.18| to |0.41|. Note that
354 the interval between the extremes of the same RP class is |1.00| (except for the lowest and highest
355 class, which have no lower and upper limit, respectively). Detailed results of the sensitivity analysis
356 are reported in SI-III

357 Insecticide application rates represent the greatest source of uncertainty in the final outcome.
358 Oscillation within the estimated prediction interval (see material and methods for details) for this
359 input parameter can cause a RP class shift for 97.6% of grid cells, with 24.4% shifting by +/- 2
360 classes. When plant interception is set to the most extreme values (0-90%), 91.6% of the grid cells
361 change to an upper or lower neighboring RP class. However, such values are unlikely to be
362 widespread over the entire productive season, therefore this assessment largely overestimates the
363 actual uncertainty due to this parameter. Uncertainty of daily rainfall intensity led to 61% of
364 potentially misclassified grid cells. The risk of misclassification due to uncertainty of the remaining
365 parameters was much lower (See SI-III for details), though for slope, shifting by up to 4 classes was
366 possible in some rare cases.

367 To conclude, our analysis identifies regions where insecticides may represent a major threat
368 to the aquatic biodiversity (Liess & von der Ohe, 2005; Vörösmarty et al., 2010). These regions
369 should be scrutinized for the actual exposure. To date the majority of studies dealing with
370 insecticide contamination of streams have been conducted on a small scale, mostly involving single
371 catchments (Verro et al., 2002). Only recently have empirical and modeling studies started to
372 extend the focus to larger areas, such as regions (Liess & von der Ohe, 2005), countries (Huber et

373 al., 2000), or continents (Kattwinkel et al., 2011, Schriever & Liess, 2007; Schriever et al., 2007).
374 This is the first attempt to assess insecticide exposure at a global scale. The separation of
375 “vulnerability” (influential environmental factors; Fig. 1) and “hazard” (anthropogenic factors; Fig.
376 2) can be used to identify appropriate strategies for managing the use of insecticides in agricultural
377 activities. Whether to mitigate hazard by making changes in the cropping system, or vulnerability
378 by introducing modifications in the local environment should be decided on a case by case basis, if
379 an actual risk at the local or regional scale has been identified.

380 The maps available in this study can increase awareness of citizens and regulators in areas
381 where the ecological effects of insecticides are likely to be significant. In addition, they could
382 prompt national or international authorities to foster targeted local investigations. In fact,
383 environmental management needs to be operatively performed at regional and local scales, but
384 investment policies can be addressed at continental or even global scales by international agencies
385 and authorities (e.g., FAO, UNEP, and OECD).

386

387 **References**

- 388 Barmaz S, Potts SG, Vighi M (2010) A novel method for assessing risks to pollinators from plant
389 protection products using honeybees as a model species. *Ecotoxicology* 19:1347–59.
- 390 Batjes NH (2006) ISRIC–WISE derived soil properties on a 5 by 5 arc–minutes global grid (version
391 1.0), ISRIC Report 2006/2.
- 392 Boatman N, Parry H, Bishop J, Cuthbertson A (2007) in *Biodiversity Under Threat.*, eds Hester R,
393 Harrison R (RSC Publishing), pp 1–32.
- 394 Boxall ABA et al. (2009) Impacts of Climate Change on Indirect Human Exposure to Pathogens
395 and Chemicals from Agriculture. *Environ Health Persp* 117:508-514.
- 396 Brown DL, Giles DK, Oliver MN, Klassen P (2008) Targeted spray technology to reduce pesticide
397 in runoff from dormant orchards. *Crop Prot* 27:545–552.

398 Burnham KP, Anderson D (2002) Model Selection and Multi-Model Inference (Springer-Verlag,
399 New York). 2nd Ed.

400 Cade BS, Terrell JW, Schroeder RL (1999) Estimating effects of limiting factors with regression
401 quantiles. Ecology 80:311–323.

402 Esty D et al. (2005) The 2005 Environmental Sustainability Index: Benchmarking National
403 Environmental Stewardship. Yale Center for Environmental Law and Policy.

404 European Commission, Joint Research Centre (2003) Global Land Cover 2000 database.

405 Finnem H, Grottenthaler W, Kühn D, Pälchen W. (2005) Bodenkundliche Kartieranleitung.
406 Schweizerbart'scheVerlagsbuchhandlung (Hannover, Germany).

407 Fleeger JW, Carman KR, Nisbet RM (2003) Indirect effects of contaminants in aquatic ecosystems.
408 Sci Total Environ 317:207–33.

409 FOCUS (2012) Generic guidance for FOCUS surface water Scenarios (version 1.2)

410 Food and Agricultural Organisation (FAO), United Nations, FAOSTAT online database,
411 <http://faostat.fao.org/> (Accessed 02/2011).

412 Food and Agricultural Organisation (FAO) & International Institute for Applied Systems Analysis
413 (IIASA) (2000) Map of global accumulated temperatures ($T_{\text{mean}} > 0 \text{ } ^\circ\text{C}$).

414 Food and Agricultural Organisation (FAO) & International Institute for Applied Systems Analysis
415 (IIASA) (2006) Mapping biophysical factors that influence agricultural production and rural
416 vulnerability, by H. van Velthuis et al., Environment and Natural Resources Series No. 11
417 (Rome, Italy).

418 Gianessi L, Reigner N (2006) Pesticide use in U.S. crop production: 2002 Insecticides and other
419 pesticides. (CropLife Foundation, Washington, D.C).

420 Grube A, Donaldson D, Kiely T, Wu L (2011) Pesticides Industry Sales and Usage - 2006 and 2007
421 Market Estimates (Washington, DC).

422 Herms DA (2004) Using degree-days and plant phenology to predict pest activity. In IPM
423 Integrated Pest Management) of Midwest Landscapes, eds Krischik V, Davidson J
424 (Minnesota Agricultural Experiment Station), pp. 49-59.

425 Huber A, Bach M, Frede HG (2000) Pollution of surface waters with pesticides in Germany:
426 modeling non-point source inputs. *Agric Ecosyst Environ* 80:191–204.

427 Ippolito A, Carolli M, Varolo E, Villa S, Vighi M (2012) Evaluating pesticide effects on freshwater
428 invertebrate communities in alpine environment: a model ecosystem experiment.
429 *Ecotoxicology* 21: 2051-2067.

430 Johnson JB, Omland KS (2004) Model selection in ecology and evolution. *Trends EcolEvol*
431 19:101–108.

432 Kattwinkel M, Kühne J-V, Foit K, Liess M (2011) Climate change, agricultural insecticide
433 exposure, and risk for freshwater communities. *Ecol Appl* 21:2068–2081.

434 Koenker R (2013) quantreg: Quantile Regression. R package version 4.98. [http://CRAN.R-](http://CRAN.R-project.org/package=quantreg)
435 [project.org/package=quantreg](http://CRAN.R-project.org/package=quantreg).

436 Koenker R, Bassett G (1978) Regression Quantiles. *Econometrica* 46:33–50.

437 Konrad CP, Brasher AMD, May JT (2008) Assessing stream flow characteristics as limiting factors
438 on benthic invertebrate assemblages in streams across the western United States. *Freshw Biol*
439 53: 1983–1998.

440 Liess M, Beketov MA (2011) Traits and stress: keys to identify community effects of low levels of
441 toxicants in test systems. *Ecotoxicology* 20:1328–1340.

442 Liess M, Von Der Ohe PC (2005) Analyzing effects of pesticides on invertebrate communities in
443 streams. *Environ Toxicol Chem* 24:954–965.

444 Mayaux P et al. (2006) Validation of the Global Land Cover 2000 Map. *IEEE Trans Geosci Remote*
445 *Sens* 44: 1728-1739.

446 National Oceanic and Atmospheric Administration (NOAA), Daily Global Historical Climatology
447 Network (GHCN Daily), <ftp://ftp.ncdc.noaa.gov/pub/data/ghcn/daily/> (Accessed 02/2011).

448 Newton I (1995) The contribution of some recent research on birds to ecological understanding. *J*
449 *Anim Ecol* 64:675–696.

450 Organisation for Economic Cooperation and Development (OECD) (1998) Report of Phase 1 of the
451 Aquatic Risk Indicators Project. (Paris, France).

452 Rasmussen JJ, Baattrup-Pedersen A, Wiberg-Larsen P, McKnight US, Kronvang B (2011) Buffer
453 strip width and agricultural pesticide contamination in Danish lowland streams: Implications
454 for stream and riparian management. *Ecol Eng* 37:1990–1997.

455 Relyea RA (2005) The impact of insecticides and herbicides on the biodiversity and productivity of
456 aquatic communities. *Ecol Appl* 15:618–627.

457 Satapornvanit K, et al. (2004) Risks of pesticide use in aquatic ecosystems adjacent to mixed
458 vegetable and monocrop fruit growing areas in Thailand. *Austral J Ecotox* 10:85–95.

459 Scharf F, Juanes F, Sutherland M, Charf FRSS, Uanes FRJ (1998) Inferring ecological relationships
460 from the edges of scatter diagrams: comparison of regression techniques. *Ecology* 79:448–
461 460.

462 Schriever CA, Liess M (2007) Mapping ecological risk of agricultural pesticide runoff. *Sci Total*
463 *Environ* 384:264–279.

464 Schriever C, von Der Ohe PC, Liess M (2007) Estimating pesticide runoff in small streams.
465 *Chemosphere* 68:2161–71.

466 Schäfer RB et al. (2007) Effects of pesticides on community structure and ecosystem functions in
467 agricultural streams of three biogeographical regions in Europe. *Sci Total Environ* 382:272–
468 285.

469 Schäfer RB et al. (2011) Effects of Pesticides Monitored with Three Sampling Methods in 24 Sites
470 on Macroinvertebrates and Microorganisms. *Environ Sci Technol* 45:1665–1672.

471 Schäfer RB et al. (2012) Thresholds for the effects of pesticides on invertebrate communities and
472 leaf breakdown in stream ecosystems. *Environ Sci Technol* 46:5134–5142.

- 473 Schäfer RB et al. (2013) How to characterize chemical exposure to predict ecologic effects on
474 aquatic communities? *Environ Sci Technol* 47:7996-8004.
- 475 Tang X, Zhu B, Katou H (2012) A review of rapid transport of pesticides from sloping farmland to
476 surface waters: Processes and mitigation strategies. *J Environ Sci* 24:351–361.
- 477 U.S. Department of Agriculture, Economic Research Centre (ERC). Real Historical Gross Domestic
478 Product (GDP) and Growth Rates of GDP for Baseline Countries/Regions (in billions of 2005
479 dollars). International Macroeconomic Data Set. Online database
480 <http://www.ers.usda.gov/Data/Macroeconomics/> (Accessed 04/2011).
- 481 Van der Werf HMG (1996) Assessing the impact of pesticides on the environment. *Agric. Ecosyst*
482 *Environ* 60:81–96.
- 483 Verro R et al. (2002) GIS-based system for surface water risk assessment of agricultural chemicals.
484 1. Methodological approach. *Environ Sci Technol* 36:1532–8.
- 485 Verro R, Finizio A, Otto S, Vighi M (2009) Predicting Pesticide Environmental Risk in Intensive
486 Agricultural Areas. I: Screening Level Risk Assessment of Individual Chemicals in Surface
487 Waters. *Environ Sci Technol* 43:522–529.
- 488 Vörösmarty CJ et al. (2010) Global threats to human water security and river biodiversity. *Nature*
489 467:555–561.
- 490 Wauchope RD (1978) The pesticide content of surface water draining from agricultural fields – a
491 review. *J Environ Qua* 7:459–72.

492

493 **Acknowledgments:**

494 We thank Marco Vighi for discussions and comments on the manuscript. This project was
495 undertaken within the topic *Chemicals in the Environment* at the Helmholtz Centre for
496 Environmental Research (UFZ), Leipzig, Germany. Collaboration among some authors was made
497 possible thanks to the scientific network SuccessioneEcologica.

498

499

500 **Figure legends**

501 **Fig. 1.** Global insecticide runoff vulnerability map.

502 The map shows the potential magnitude of insecticide runoff regardless of the actual agricultural
503 activity and incorporates all natural variables included in the model to calculate RP. Class
504 boundaries have been assigned ex-post according to the distribution of the values (see Materials and
505 Methods).

506 **Fig. 2.** Global insecticide runoff hazard map.

507 The map considers all variables of the RP model that are under human control and are connected to
508 agricultural activities. Class boundaries have been assigned ex-post according to the distribution of
509 the values (see Materials and Methods). Grey areas indicate the absence of any relevant agricultural
510 activity.

511 **Fig. 3.** Global insecticide RP map.

512 The map shows the spatial distribution of potential insecticide runoff to stream ecosystems.
513 According to this estimation, the surface waters in 43% of the total global land area are potentially
514 subject to insecticide load as a consequence of current agricultural practices. The class boundaries (-
515 3;-2;-1;0) are the same as those used in previous studies (Kattwinkel et al., 2011). Grey areas
516 indicate the absence of any relevant agricultural activity.

517

518

519

Figure 1
[Click here to download Figure: Fig.1.pdf](#)

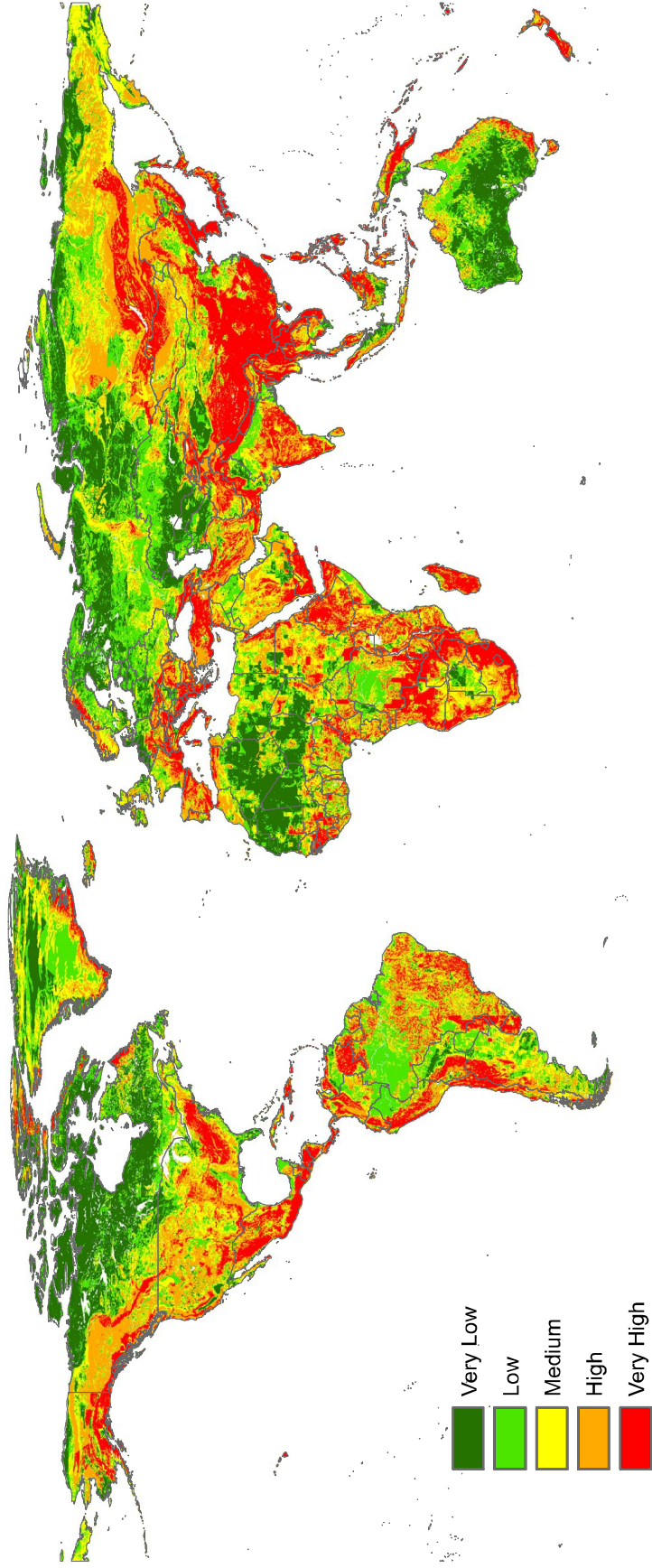


Figure 2
[Click here to download Figure: Fig.2.pdf](#)

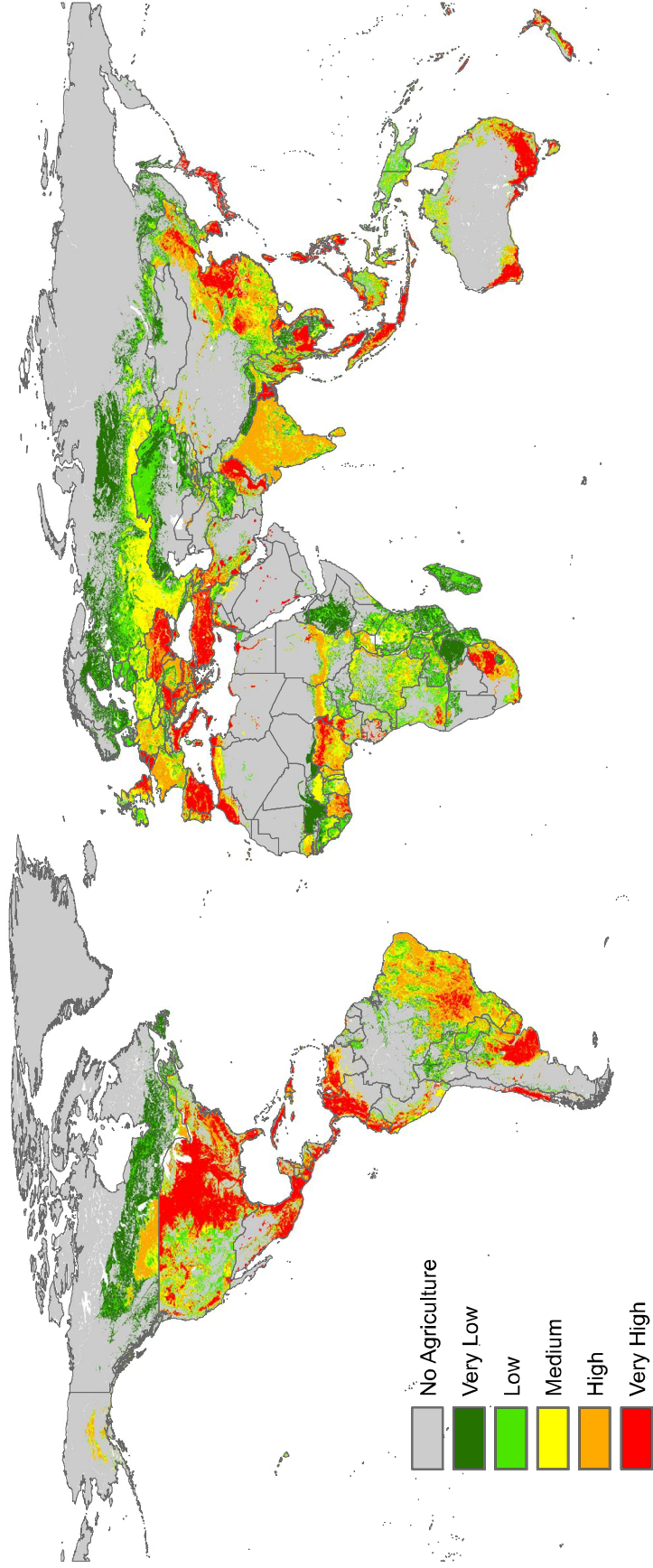
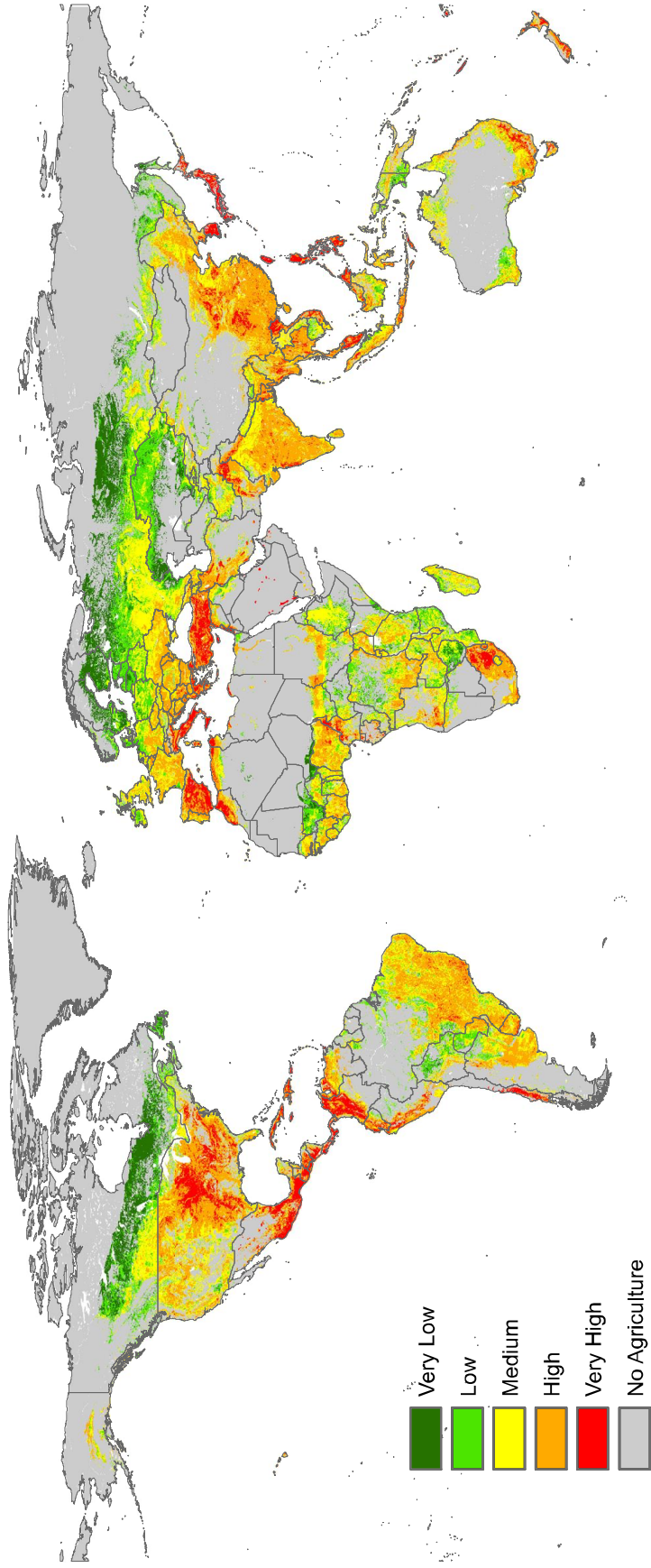


Figure 3
[Click here to download Figure: Fig.3.pdf](#)



Supplementary Material 1

[Click here to download Supplementary Material: SI I.pdf](#)

Supplementary Material 2

[Click here to download Supplementary Material: SI II.pdf](#)

Supplementary Material 3

[Click here to download Supplementary Material: SI III.pdf](#)

Supplementary Material 4

[Click here to download Supplementary Material: SI IV.pdf](#)